nature climate change

ARTICLES

https://doi.org/10.1038/s41558-020-0747-7

Diminishing CO_2-driven gains in water-use efficiency of global forests

Mark A. Adams[1,2,4] ✉, **Thomas N. Buckley**[3,4] and **Tarryn L. Turnbull**[1,2,4]

There is broad consensus that, via changes in stomatal conductance, plants moderate the exchanges of water and carbon between the biosphere and atmosphere, playing a major role in global hydroclimate. Tree rings record atmospheric CO_2 concentration (c_a) and its isotopic composition ($^{13}C/^{12}C$)—mediated by stomatal and photosynthetic influences—that can be expressed in terms of intrinsic water-use efficiency (W). Here, we compile a global W dataset based on 422 tree-ring isotope series and report that W increased with c_a over the twentieth century, but the rates of increase (dW/dc_a) declined by half. Angiosperms contributed more than gymnosperms to the slowdown, and in recent decades, dW/dc_a for angiosperms was close to zero. dW/dc_a varies widely across climatic regions and reflects pauses in emissions during the Great Depression and after World War II. There is strong spatial variability in climate forcing via an increasing W, which is weakening globally with time.

Variation in stomatal conductance (g_s) at temporal scales ranging from seconds to centuries plays a major controlling role in the rates of exchange of water and carbon between the biosphere and atmosphere[1,2]. Discrimination against $^{13}CO_2$ relative to $^{12}CO_2$ during inward diffusion from the atmosphere to leaves during photosynthesis depends sufficiently strongly on g_s such that the latter can be approximated via the $^{13}C/^{12}C$ ratios of plant tissues ($\delta^{13}C = [(^{13}C/^{12}C)_{sample}/(^{13}C/^{12}C)_{standard}]$). $\delta^{13}C$ of tree-ring tissue is widely used as a time-integrated (usually annual) measure of g_s. As g_s controls both the inward diffusion of CO_2 and the outward diffusion of H_2O (to the atmosphere), a common definition of intrinsic water-use efficiency (W or iWUE (Frank et al.[3] and van der Sleen et al.[4])) is:

$$W = A/g_s = (c_a - c_i)/1.6 = c_a(1 - c_i/c_a)/1.6 \qquad (1)$$

where A is the net photosynthesis, and c_a and c_i are the mole fractions of CO_2 in ambient air and intercellular airspaces, respectively. The ratio c_i/c_a can be estimated from Δ, the $\delta^{13}C$ of wood corrected for the isotopic composition of atmospheric CO_2. Reductions in g_s are broadly associated with increases in W, and can substantially influence rainfall and runoff at regional and continental scales[5–9] via concomitant reductions in whole-tree transpiration.

Increases in W are fundamental to many aspects of global carbon and water cycles. For example, Keeling et al.[10] recently showed that decreases in $^{13}C/^{12}C$ ratios of atmospheric CO_2 (the ^{13}C-Suess effect)—which is mostly attributed to the effects of additions of CO_2 derived from fossil fuel—can only be fully explained by including putative changes in the stomatal conductance and W of tropical forests. The theoretical importance of increases in c_a that lead to an increased W has been recognized for decades[11] and is now backed by a large body of evidence from flux measurements, free-air CO_2-enrichment experiments, tree-ring studies and hundreds of leaf-level studies[3,4,12,13]. We have, however, lacked a comprehensive spatiotemporal analysis of the variation in c_a–W relationships across the globe.

The need for a more detailed knowledge of the c_a–W relationship is underlined by the importance of W as a driver (or 'physiological forcer') of long-term hydrological cycles, along with current rainfall and temperature (via evaporative cooling)[3–9,14–18]. Mounting evidence shows that physiological forcings strongly influence rainfall within large tropical river basins at a range of timescales[6–9], and are increasingly recognized as drivers of global climate[9,14–16]. Researchers[17] have called for plant-centric measures to be incorporated in models as a way of to improve climate predictions.

As of early 2018, the International Tree-Ring Data Bank contained 29 tree-ring records of carbon isotopes ('isotope series') of varying duration, with a clear bias to Europe and North America. To greatly expand this resource, we extracted and collated from the literature all the available long-term tree-ring isotope series, and accommodated for variation among the studies in how carbon isotope or W data are reported. We then estimated W from isotopic discrimination and calculated the rate of change of W with respect to c_a (dW/dc_a) (Methods). As a plant-derived measure of the effect of c_a on hydrological cycles, dW/dc_a has not been rigorously assessed across the globe, despite frequent observations that W has mostly increased with c_a (for example, Frank et al.[3], van der Sleen et al.[4] and Keenan et al.[12]). We tested how a rising c_a affects W, and if dW/dc_a shows a dependence on ecosystem properties, such as climate and dominant plant group (angiosperms versus gymnosperms). Our analysis included the modelled effects of century-scale changes in photosynthesis, mesophyll conductance and photorespiration (Methods). We also tested if climate-related biases in photosynthetic responses to c_a influenced patterns in W (Methods).

We found tree-ring isotopic data from which we could calculate W for all broad (Köppen) climatic zones and continents, except Antarctica (Fig. 1, Extended Data Fig. 1, Supplementary Tables 1 and 2). All major forested areas of the globe are represented and, although we compiled studies that include data reaching back several centuries, we only extracted isotopic data back to 1850 (Extended Data Fig. 1). There remains an obvious sampling bias to the Northern Hemisphere and to Central Europe, Scandinavia,

---

[1]Department of Chemistry and Biotechnology, Faculty of Science, Engineering and Technology, Swinburne University of Technology, Melbourne, Victoria, Australia. [2]School of Life and Environmental Sciences, University of Sydney, Camperdown, New South Wales, Australia. [3]Department of Plant Sciences, College of Agricultural and Environmental Sciences, University of California, Davis, Davis, CA, USA. [4]These authors contributed equally: Mark A. Adams, Thomas N. Buckley, Tarryn L. Turnbull. ✉e-mail: maadams@swin.edu.au

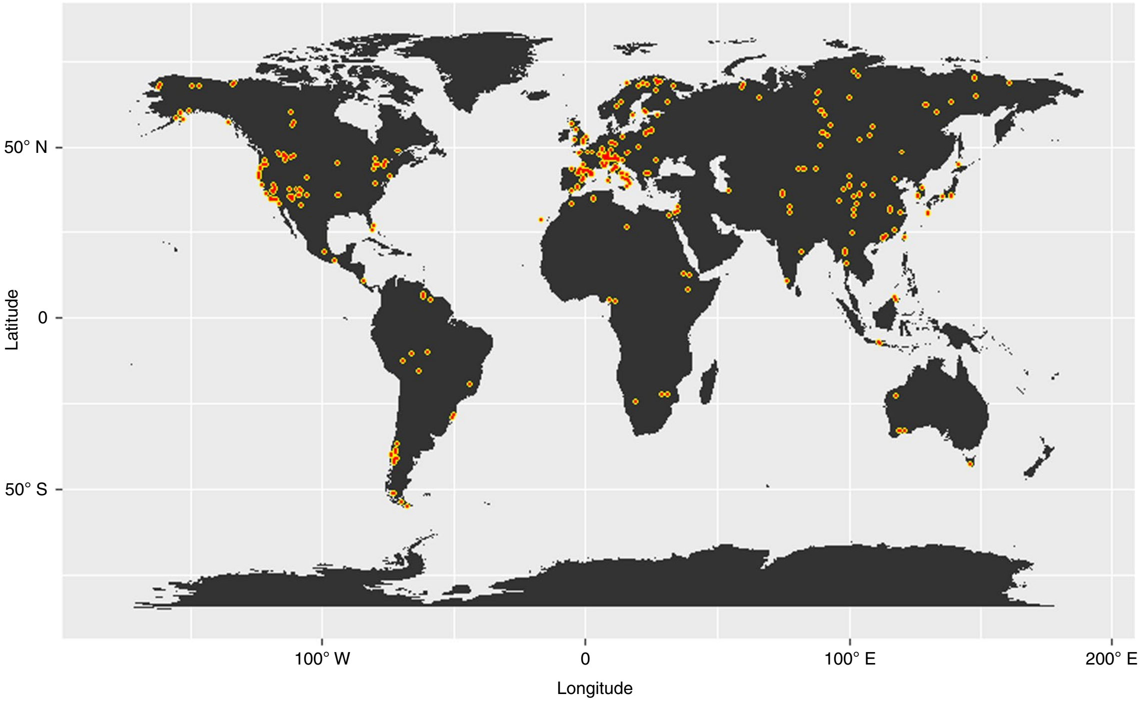

Fig. 1 | Geographical locations of 422 tree-ring isotope series that contain data from the period 1851–2015. All the data are extracted from published literature.

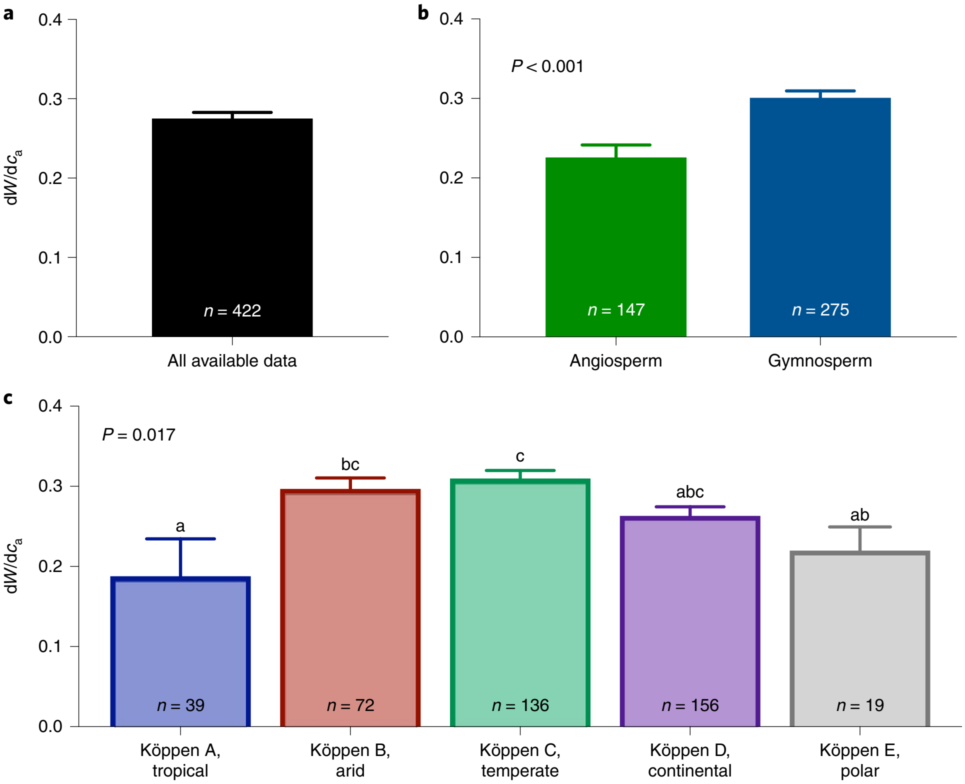

Fig. 2 | d*W*/dc_a based on 422 tree-ring isotope series from the period 1851–2015. a, All data (Supplementary Table 1). **b**, Data split into angiosperms and gymnosperms. **c**, Data split by Köppen climate zone. The data shown are mean and standard error of the mean (s.e.m.), and the number of individual species. Comparisons are based on linear mixed models with study as a random factor. Columns marked with the same letter are not significantly different ($P < 0.05$).

North America and East Asia (Fig. 1). Africa and South America are represented mainly via more coastal sites. Oceania and Central Asia are poorly represented.

We present two estimates of dW/dc_a (Supplementary Table 1): one based the on traditional methods for the calculation of W (equation (2)) and a second based on the assumed influences on W of mesophyll conductance and photorespiration (and their change over the past century), and photosynthetic responses to c_a (equation (3)). As we show in Extended Data Fig. 2, the combined effect of these is to change the intercepts and slopes of linear relations between c_a and W. We also confined the majority of our detailed statistical analyses to the twentieth century. In the following discussion, we focus only on estimates of W that are corrected for these combined influences.

For all isotope series within the period 1851–2015, the average rate of increase in W with respect to c_a (unitless, ppm ppm^{-1}) was 0.28 (Fig. 2a). For context, during the period 1901–2000, c_a rose from ~297 to ~370 ppm and W increased ~50% (Fig. 3a). In a few cases, dW/dc_a was negative (that is, W declined with c_a), but overall dW/dc_a was normally distributed around its mean (Extended Data Fig. 3a). For 376 of the 422 individual isotope series, W showed highly significant ($P < 0.01$), positive linear relations with c_a (Extended Data Fig. 3a,c), there were significant relations ($P < 0.05$) for a further 20 and the remainder (26) showed no relationship. The rise in c_a explains the majority of the observed change in W ($R^2 > 0.5$, Extended Data Fig. 3) for >72% of all the isotope series.

Gymnosperms ($dW/dc_a = 0.30$) showed faster rates of change in W with c_a than angiosperms ($dW/dc_a = 0.23$; Fig. 2b) over this period (1851–2015). The mean dW/dc_a was significantly less in the tropics (0.19, Köppen zone A; Fig. 2c) than in Köppen zones B (0.30, arid) and C (0.31, temperate), or in zone D (0.26, continental). Although relatively few in number, studies from polar climates accord with those from other regions ($dW/dc_a \approx 0.22$). Further exploring climate influences on dW/dc_a (Extended Data Fig. 4a–o), we found that across the globe, rainfall accounted for around 10% of the variation in angiosperm dW/dc_a, which fell by about 0.1 (or 36% of the twentieth-century mean dW/dc_a) per 1,000 mm of additional rainfall. Stronger effects on dW/dc_a may be evident within regions where the range in rainfall is large (see Adams et al.[19] for a recent study in the tropics). For gymnosperms, potential evaporation, temperature, vapour pressure and radiation all show significant positive relations with dW/dc_a (Extended Data Fig. 4l–o).

Restricting the analysis to isotope series that spanned the twentieth century (that is, from trees that were »100 years of age by 2,000 (Methods)) clearly revealed the slowing rate of change in W with c_a (Fig. 3). A second-order polynomial provided a very strong fit for all twentieth-century data (Fig. 3a). When we split the century data into those pre- and post-1965 (a commonly used reference point for the subsequent rapid rises in c_a), then the calculated mean dW/dc_a for 1901–1965 is 0.34, whereas that for 1966–2000 is 0.25—a reduction of around 27% (Fig. 3b). There was a slightly greater variation in dW/dc_a for angiosperms than gymnosperms in the period 1901–1965, but angiosperms contributed more strongly to the overall slowing of dW/dc_a in the latter decades of the twentieth century and the first decade of the twenty-first century (Fig. 3c).

When the data were binned using a range of time windows (Fig. 4a–c), there was a consistent reduction in dW/dc_a throughout the twentieth century (Supplementary Table 2). This approach also reveals the greater variability in data pre-1957 (see Methods for a discussion of the potential causes of uncertainty). Using a ten-year bin shows a significantly greater dW/dc_a in the periods 1920–1930 and 1940–1950 than in other decades of the twentieth century (Fig. 4d). Pauses in the rise of c_a in (1) the Great Depression due to the downturn in economic production and energy use[20] and (2) during and after World War II (including land abandonment) have been previously analysed[20–22]. During these periods, slower rates of increase in c_a led to proportionally greater rates of change in W. In contrast, the persistent decline in decadal-scale dW/dc_a since 1965 corresponds with the period of exponential increases in CO_2 emissions and in c_a (ref. [22]. When further partitioned, the data show that from 1950 to 1990, decadal mean dW/dc_a were not significantly different between gymnosperms and

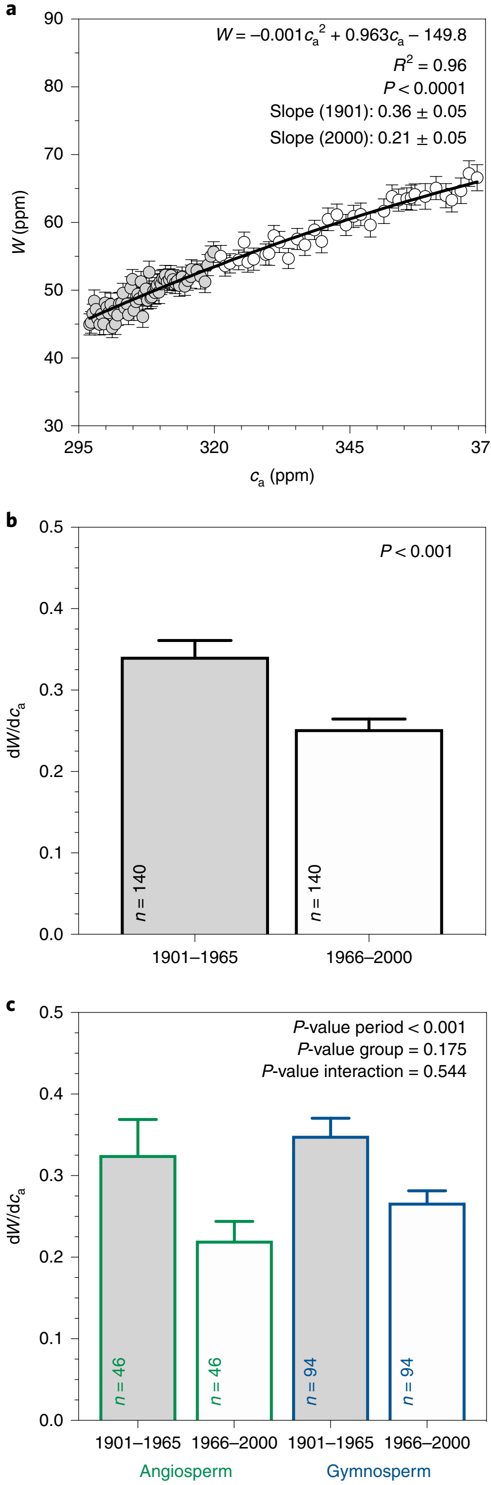

Fig. 3 | Changes in sensitivity of W to changes in c_a over time. Based on 140 tree-ring isotope series in which each series spans the 1901–2000 period (Supplementary Table 1). **a**, Second-order polynomial model of changes in mean annual W (± s.e.m.) with c_a for 1901–2000 data. **b**, Mean and s.e.m. of dW/dc_a for the 1901–1965 and 1966–2000 subsets. **c**, Mean and s.e.m. of dW/dc_a for angiosperms and gymnosperms. Period comparisons are based on data for 1901–1965 versus 1966–2000, while group comparisons are angiosperms versus gymnosperms. The comparisons in **b** and **c** are based on linear mixed models with study as a random factor.

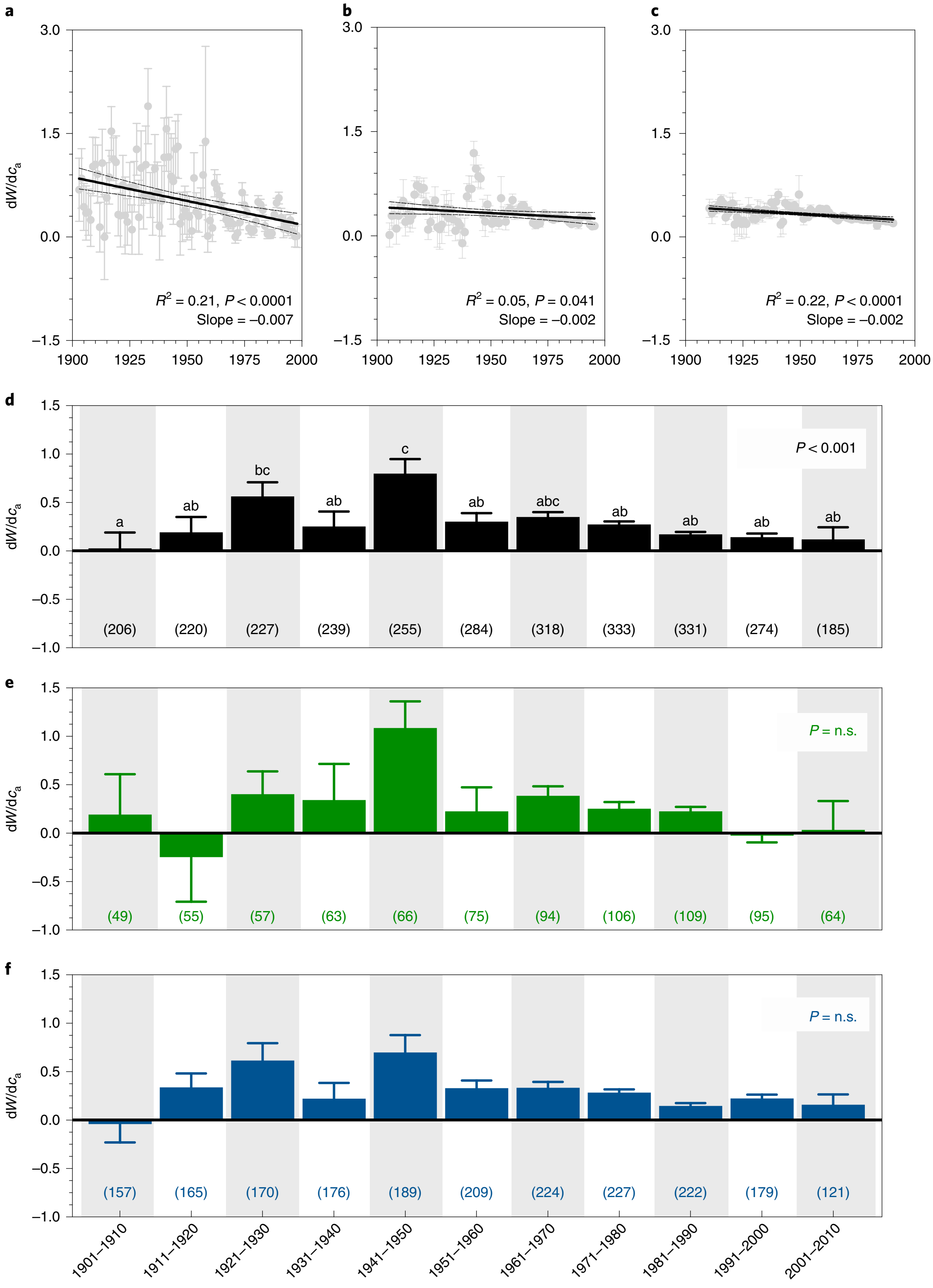

Fig. 4 | Patterns in d*W*/dc_a. The graphs are based on 422 tree-ring isotope series that contain data within the period 1851–2015 (Supplementary Table 2). **a**–**c**, Linear regressions of moving averages of the dataset in which data is binned by 5-year intervals (**a**), 10-year intervals (decadal) (**b**) and 20-year intervals (**c**). **d**–**f**, Ten-year (decadal) mean, s.e.m. and number of replicates in parentheses for all data combined (columns marked by the same letter are not signifcantly different ($P < 0.05$)) (**d**), angiosperms (**e**) and gymnosperms (**f**). **d**–**f**, *P* values are from linear mixed models with study as a random factor, d*W*/dc_a were significantly different among decades only when all the data were combined (**d**) and d*W*/dc_a were not significantly different (n.s.) for angiosperms and gymnosperms ($P < 0.05$), except in 1991–2000 when $P = 0.021$.

angiosperms. Only since 1990 has the mean decadal d*W*/dc_a for gymnosperms been significantly greater ($P = 0.021$) than that for angiosperms (Fig. 4e,f).

It is unsurprising that *W* has increased with c_a given the results of enrichment experiments (for example, free-air CO_2-enrichment studies) that show reductions in both stomatal conductance and photosynthetic capacity[23] at individual sites and collectively. However, our global dataset indicates that the average dW/dc_a has declined by ~42%, from about +0.36 in 1901 to about +0.21 in 2000 (Fig. 3a). Applying these values to equations (9–12) (Methods) suggests that, although the ratio of photosynthetic capacity (that is, the light- and CO$_2$-saturated photosynthetic rate, A_{max}) to stomatal conductance to CO$_2$ (g_{sc}) has increased with c_a over the twentieth century (that is, d(A_{max}/g_{sc})/dc_a was positive), the rate of increase in this ratio has slowed markedly. It declined by ~75% (from ~2.0 to ~0.5) assuming carboxylation-limited conditions, or by ~52% (from ~0.74 to ~0.36), assuming regeneration-limited conditions. Extending this analysis to account for the widest possible range in the response of assimilation rate to c_a (which affects the calculation of W from isotopes[10]; equation (3)) suggests that d(A_{max}/g_{sc})/dc_a declined by between 46 and 99% over the twentieth century. The true change is probably somewhere between these limits.

Thus, stomatal conductance declined faster than photosynthetic capacity—but the rate of increase in A_{max}/g_{sc} slowed over the past half-century. The first inference (that A_{max}/g_{sc} increased) is consistent with a meta-analysis of CO$_2$-enrichment experiments using trees[24], which found that g_{sc} typically declined by ~20% with doubling of c_a, whereas A_{max} declined by a much smaller amount, 0–10%. The second inference (that the rate of increase in A_{max}/g_{sc} slowed) is consistent with the common finding that a sustained exposure to elevated CO$_2$ can lead to nutrient limitation, given that A_{max} depends chiefly on nitrogen (N) supply[13,23,24].

A recent detailed study of North American coniferous forests[25] used a dual-isotope approach (δ^{13}C and δ^{18}O) to separate the effects of c_a on stomatal conductance and photosynthetic capacity. The data from that study suggest that the photosynthetic capacity was more important than stomatal conductance to contemporary changes in W, albeit this pattern disappeared or reversed on low-rainfall sites. Although some leaf-level studies suggest that angiosperm stomatal conductance is more responsive to c_a than that of gymnosperms[26,27] (Fig. 4), there are open questions about the respective responses of photosynthetic capacity. In this context, another meta-analysis revealed recent significant declines in leaf N across the globe, to such an extent that the authors ascribed them as indications of ecosystem oligotrophication[28]. As the authors noted[28], reductions in leaf N as a result of rising c_a are almost certainly associated with reductions in photosynthetic capacity (also see Ainsworth and Long[23] and Oren et al.[24]). Conversely, disturbances often enhance soil water and nutrient availability (for example, via removal of overstorey or the encouraged growth of N-fixing plants), and have major effects on W (ref. [29]). Our model and empirical evidence aligns with considerable other recent data. Collectively, these highlight the need for much more analysis, and greater understanding, of the relationship of W to nutrient and water availability across the Earth's forests.

Irrespective of the cause(s) of the slowdown in the acclimation of water-use efficiency, isotope series data derived from tree rings clearly suggest there are limits to CO$_2$-driven changes in hydrological cycles of the world's mature forests. Proposed changes in transpiration as a result of stomatal closure and reduced g_s, which include increases in runoff at continental scales[3–7], may slow, or even cease, as trees encounter intrinsic physiological limits to their capacity to respond to additional CO$_2$.

The data compiled here offer a complementary perspective on W to that obtained by other methods, such as eddy flux and remote sensing. The overall slowing in c_a-driven changes in W—which for angiosperms resulted in dW/dc_a being close to zero for 1991–2000 (Fig. 4e)—has not been universally recognized. In part, this lack of recognition reflects the relatively short duration (~30 years) of flux stations and networks and the confounding influences of climate and disturbance on the consequent data. Reported recent increases in the W of North America forests[12] were, for example, based on flux analyses of duration 5–15 years. However, using measurements of the ^{13}C/^{12}C ratio of the atmospheric CO$_2$, Peters et al.[1] reported that in the decade 2001–2011, increases in W were, in fact, temporary and coincided with severe droughts in Europe, Russia and the United States. Similarly, Yang et al.[30] recently reported both short-term (year-to-year) increases and decreases in W with drought in recent decades, depending on the prevailing climate (for example, arid versus semi-arid or subhumid). There is obvious potential to use tree-ring data as a means of to validate flux data, and vice versa.

We thus argue that the ability to reliably discern c_a-driven changes in W from those due to other influences currently rests at the decadal scale, as used here. A recent illustration of the year-to-year variability in W derived from flux measurements (Fig. 8 in Tang et al.[31]) highlights the difficulty of determining the direction and size of changes in W from flux studies alone. Although isotope-derived measures of W based on tree rings also need careful interpretation (see Esper et al.[32] for a discussion of relevant considerations), they offer a time-integrated (and long-term) measure not easily obtained by other means.

Tree-ring data are vital to understanding past climates as well as to predict future climates across the globe. As Marvel et al.[5] surmised, tree-ring records are the basis for reconstructing temperature and hydroclimatic variables at annual and seasonal resolutions within the twentieth century. Tree-ring records underpin the widely used current measures of drought, such as the Palmer Drought Severity Index[2], which have been developed on a grid basis for large regions of the globe[33]. Accordingly, there are very substantial efforts to build global grid-based measures of W (refs [31–33]) because the responses of stomatal conductance to c_a help to determine the daily rainfall[4–6] for large basins, such as the Amazon, as well as for regional- and continental-scale runoff and water balances at timescales that range from days to centuries[3,33]. The compiled data reported here can be used to calibrate predictive models of thermal regimes, which include heatwaves[17,18], and help to meet calls for a plant-based, integrative metric of the long-term influence of c_a on the transfer of water from terrestrial systems to the atmosphere[17]. The revealed, long-term slowing rate of the increase in W is an essential baseline against which to compare reports of increasing W based in selected time periods[12].

For very large areas of the globe, however, tree-ring data remain scant. These includes major river basins, such as the Congo and Amazon, land masses, such as Papua New Guinea and Australia, and all of Central Asia. Redressing these gaps, as well as a more detailed exploration of nutrient and water effects on the ^{13}C/^{12}C isotopic ratios in tree rings and a better quantification of the contributions of photosynthetic capacity and stomatal conductance to W, are obvious global priorities.

Online content

Any methods, additional references, Nature Research reporting summaries, source data, extended data, supplementary information, acknowledgements, peer review information; details of author contributions and competing interests; and statements of data and code availability are available at https://doi.org/10.1038/s41558-020-0747-7.

Received: 29 July 2019; Accepted: 6 March 2020;
Published online: 27 April 2020

References

1. Peters, W. et al. Increased water-use efficiency and reduced CO$_2$ uptake by plants during droughts at a continental scale. *Nat. Geosci.* **11**, 744–748 (2018).
2. Skinner, C. B. et al. The role of plant CO$_2$ physiological forcing in shaping future daily-scale precipitation. *J. Clim.* **30**, 2319–2340 (2017).
3. Frank, D. C. et al. Water-use efficiency and transpiration across European forests during the Anthropocene. *Nat. Clim. Change* **5**, 579–583 (2015).
4. van der Sleen, P. et al. No growth stimulation of tropical trees by 150 years of CO$_2$ fertilization but water-use efficiency increased. *Nat. Geosci.* **8**, 24–28 (2015).
5. Marvel, K. et al. Twentieth-century hydroclimate changes consistent with human influence. *Nature* **569**, 59–65 (2019).

6. Betts, R. A. et al. Projected increase in continental runoff due to plant responses to increasing carbon dioxide. *Nature* **448**, 1037–1041 (2007).
7. Kooperman, G. J. et al. Forest response to rising CO_2 drives zonally asymmetric rainfall change over tropical land. *Nat Clim. Change* **8**, 434–440 (2018).
8. Richardson, T. B. et al. Carbon dioxide physiological forcing dominates projected eastern Amazonian drying. *Geophys. Res. Lett.* **45**, 2815–282 (2018).
9. Langenbrunner, B., Pritchard, M. S., Kooperman, G. J. & Randerson, J. T. Why does Amazon precipitation decrease when tropical forests respond to increasing CO_2? *Earths Future* **7**, 450–468 (2018).
10. Keeling, R. F. et al. Atmospheric evidence for a global secular increase in carbon isotopic discrimination of land photosynthesis. *Proc. Natl Acad. Sci. USA* **114**, 10361–10366 (2017).
11. Franks, P. J. et al. Sensitivity of plants to changing atmospheric CO_2 concentration: from the geological past to the next century. *New Phytol.* **197**, 1077–1094 (2013).
12. Keenan, T. F. et al. Increase in forest water-use efficiency as atmospheric carbon dioxide concentrations rise. *Nature* **499**, 324–327 (2013).
13. Norby, R. J. & Zak, D. R. Ecological lessons from free-air CO_2 enrichment (FACE) experiments. *Ann. Rev. Ecol. Evol. Syst.* **42**, 181–203 (2011).
14. Cao, L. et al. Importance of carbon dioxide physiological forcing to future climate change. *Proc. Natl Acad. Sci. USA* **107**, 9513–9518 (2010).
15. de Boer, H. J. et al. Climate forcing due to optimization of maximal leaf conductance in subtropical vegetation under rising CO_2. *Proc. Natl Acad. Sci. USA* **108**, 4041–4046 (2011).
16. Richardson, T. B., Forster, P. M., Andrews, T. & Parker, D. J. Understanding the rapid precipitation response to CO_2 and aerosol forcing on a regional scale. *J. Clim.* **29**, 583–594 (2016).
17. Skinner, C. B., Poulsen, C. J. & Mankin, J. S. Amplification of heat extremes by plant CO_2 physiological forcing. *Nat. Commun.* **9**, 1094 (2018).
18. Kala, J. et al. Impact of the representation of stomatal conductance on model projections of heatwave intensity. *Sci. Rep.* **6**, 23418 (2016).
19. Adams, M. A., Buckley, T. N. & Turnbull, T. L. Rainfall drives variation in rates of change in intrinsic water use efficiency of tropical forests. *Nat. Commun.* **10**, 3661 (2019).
20. Estrada, F., Perron, P. & Martinez-López, B. Statistically derived contributions of diverse human influences to twentieth-century temperature changes. *Nat. Geosci.* **6**, 1050–1055 (2013).
21. Bastos, A. et al. Re-evaluating the 1940s CO_2 plateau. *Biogeosci.* **13**, 4877–4897 (2016).
22. Hofmann, D., Butler, J. H. & Tans, P. P. A new look at atmospheric carbon dioxide. *Atmos. Environ.* **43**, 2084–2086 (2009).
23. Ainsworth, E. A. & Long, S. P. What have we learned from 15 years of free-air CO_2 enrichment (FACE)? A meta-analytic review of the responses of photosynthesis, canopy properties and plant production to rising CO_2. *New Phytol.* **165**, 351–372 (2005).
24. Oren, R. et al. Soil fertility limits carbon sequestration by forest ecosystems in a CO_2-enriched atmosphere. *Nature* **41**, 469–472 (2001).
25. Guerrieri, R. et al. Disentangling the role of photosynthesis and stomatal conductance on rising forest water-use efficiency. *Proc. Natl Acad. Sci. USA* **116**, 16909–16914 (2019).
26. Lin, Y.-S. et al. Optimal stomatal behaviour around the world. *Nat. Clim. Change* **5**, 459–464 (2015).
27. Klein, T. & Ramon, U. Stomatal sensitivity to CO_2 diverges between angiosperm and gymnosperm tree species. *Funct. Ecol.* **33**, 1411–1424 (2019).
28. Craine, J. M. et al. Isotopic evidence for oligotrophication of terrestrial ecosystems. *Nat. Ecol. Evol.* **2**, 1735–1744 (2018).
29. Donohue, R. J., Roderick, M. L., McVicar, T. R. & Yang, Y. A simple hypothesis of how leaf and canopy-level transpiration and assimilation respond to elevated CO_2 reveals distinct response patterns between disturbed and undisturbed vegetation. *J. Geophys. Res. Biogeosci.* **122**, 168–18415 (2017).
30. Yang, Y. et al. Contrasting responses of water use efficiency to drought across global terrestrial ecosystems. *Sci. Rep.* **6**, 23284 (2016).
31. Tang, X. et al. How is water-use efficiency of terrestrial ecosystems distributed and changing on Earth? *Sci. Rep.* **4**, 7483 (2014).
32. Esper, J. et al. Low-frequency noise in $\delta^{13}C$ and $\delta^{18}O$ tree ring data: a case study of *Pinus uncinata* in the Spanish Pyrenees. *Glob. Biogeochem. Cycles* **24**, GB4018 (2010).
33. Jasechko, S. et al. Terrestrial water fluxes dominated by transpiration. *Nature* **496**, 347–350 (2012).

Methods

Data collection and analysis. The data compiled and synthesized here comprise 422 independent tree-ring isotope series (each series being an individual species at a given site) from 179 published studies across the globe (Extended Data Fig. 1, Supplementary Table 1). It includes 134 different tree species; 61 species (from 34 genera) of angiosperms and 73 species (from 22 genera) of gymnosperms, and covers each Köppen climate zones.

To compile our database, we first identified literature that contained any form of data that pertained to tree-ring ^{13}C isotope series between 1850 and 2015 by screening the Web of Science and Google Scholar search engines using the keywords dendrochron* (where the asterisk is a wildcard), cellulose, tree ring, carbon isotope discrimination, ^{13}C, water-use efficiency, tropic*. We also screened citations within these publications for any additional isotope series that may not have been identified by the search-engine screen.

Data were extracted from this published literature in several ways. When originally tabulated, we manually recorded the data as provided into our database. When presented in graphical form, we manually digitized each individual isotope series using the digitizing software GraphClick (version 3.0.2, Arizona software). In a few cases, we obtained data from the original authors, mainly when a component of W (for example, ^{13}C/^{12}C for wood, Δ or W itself) was unavailable in the published literature, or if the data published in the literature were pooled across species or sites. Finally, when data were lodged with International Tree-Ring Databank (NOAA), it was downloaded and attributed according to its original publication, as described in the International Tree-Ring Data Bank protocol. In every case, we also extracted all the additional supporting data, such as species identity, climate and location (Supplementary Table 1). We used location (latitude and longitude of each site) to identify the mean annual precipitation (mm)), mean annual potential evaporation, mean annual temperature and vapour pressure (Climatic Research Unit, https://crudata.uea.ac.uk/cru/data/hrg/), radiation (WorldClim V2.0) and confirm Köppen climate classification (Department of Environment, Water and Nature Protection). We have lodged the data for W in a publicly available repository (https://doi.org/10.5281/zenodo.3693240).

Atmospheric CO$_2$ concentration and δ^{13}C record. We used annual averages of c_a and the δ^{13}C of atmospheric CO$_2$ from McCarroll and Loader[34] (data available for 1850–2003). This dataset owes much to the work of Robertson et al.[35]. There are obvious uncertainties in the pre-1957 estimates of c_a, in particular owing to the combination[35] of a range of different estimates to arrive at an average figure for the globe. Further uncertainty is present as a result of the seasonal variation in c_a (also see Hofmann et al.[22]), as well as its latitudinal variation. We did not attempt to correct c_a according to the geographical location or seasonality of growth. Doing so could help reduce some of the observed variation in dW/dc_a. The gymnosperm dominance of northerly latitudes, with greater seasonal amplitude in c_a, relative to the more abundant angiosperms in temperate and tropical regions, with a more constant c_a, may also contribute to the patterns shown in Fig. 3c. To account for such sources of potential variation was beyond the scope of our study.

We extended the 1850–2003 dataset to 2004–2015 using monthly averages from the South Pole (http://scrippsco2.ucsd.edu/data/atmospheric_co2/spo) as described by Keeling et al.[36]. The compiled atmospheric δ^{13}C (δ^{13}C$_{\mathrm{atm}}$) record contains an artefactual discrete shift between 2003 and 2004 because the data before 2004 are from ice cores in Antarctica, at 66° 44′ S, rather than from the South Pole, and there is a small latitudinal trend in δ^{13}C$_{\mathrm{atm}}$. To remove that artefact, we fitted a second-order polynomial for δ^{13}C$_{\mathrm{atm}}$ versus year to data from 1992 to 2015, and used the resulting equation (δ^{13}C$_{\mathrm{atm}}$ = 0.0004 yr^2 – 1.6307 yr + 1,650.3; R^2 = 0.992) to produce a smoothed trend for δ^{13}C$_{\mathrm{atm}}$ in the period 2004–2015 inclusive.

Calculation of intrinsic *W* from isotopic data. Equation (1) shows a simple form of calculation of W from c_i/c_a, as estimated from δ^{13}C (or Δ). This widely used traditional approach[37] omits the effects of mesophyll conductance and photorespiration and can be rearranged:

$$c_{\mathrm{i}}/c_{\mathrm{a}} = (\Delta - a)/(b - a) \tag{2}$$

where a = 4.4‰ and b = 27‰. We computed W using equation (2) to facilitate comparison with previous literature.

However, we followed Keeling et al.[10] and included the effects of mesophyll conductance and photorespiration in our primary analysis of W:

$$c_{\mathrm{i}}/c_{\mathrm{a}} = (\Delta - a + (b - a_{\mathrm{m}})(A/c_{\mathrm{a}})/g_{\mathrm{m}} + f\Gamma_{*}/c_{\mathrm{a}})/(b - a) \tag{3}$$

where a (4.4‰) and b (30‰) are discrimination coefficients for stomatal diffusion and CO$_2$ fixation by Rubisco (ribulose-1,5-bisphosphate carboxylase/oxygenase), a_m = 1.8‰, f is the discrimination due to photorespiration (12‰), g_m is the mesophyll conductance to CO$_2$ (0.2 mol m^{-2} s^{-1}) and Γ_* is the photorespiratory CO$_2$ compensation point (43 ppm).

Equation (3) requires a value for the ratio of photosynthesis to c_a, A/c_a, which typically declines as c_a increases. We represented this decline using equation (4):

$$A/c_{\mathrm{a}} = (A/c_{\mathrm{a}})_{280}(c_{\mathrm{a}}/280)^{\beta} \tag{4}$$

where $(A/c_a)_{280}$ is the pre-industrial value of A/c_a (at c_a = 280 ppm), β = ln(DR)/ln(2) – 1 and DR is the doubling ratio (the proportion by which A increases with a doubling of c_a). Again following Keeling et al.[10], we assumed DR = 1.45, (that is, A increases by 45% with the doubling of c_a from 280 to 560 ppm).

Estimation of Δ. Equations (2) and (3) both require values for Δ, the stable C isotope ratio of wood cellulose (δ^{13}C$_{\mathrm{wood}}$ (‰)) corrected for the isotopic composition of atmospheric CO$_2$ (δ^{13}C$_{\mathrm{atm}}$ (‰)). In a few cases in which whole wood was used for the isotopic analysis, we applied simple corrections:

$$\Delta = (\delta^{13}\mathrm{C_{atm}} - \delta^{13}\mathrm{C_{wood}})/(1 + 0.001 \times \delta^{13}\mathrm{C_{wood}}) \tag{5}$$

In many articles, authors do not present Δ, but instead provide data in one of several different forms: (1) uncorrected δ^{13}C$_{\mathrm{wood}}$, (2) δ^{13}C$_{\mathrm{wood}}$ corrected using a pre-industrial value for δ^{13}C$_{\mathrm{atm}}$ (−6.4‰), (3) W calculated from c_a and Δ using equations (1) and (2) or (4) c_i calculated from c_a and Δ using equation (2).

We converted these inputs into a common Δ basis as follows:

- For (1), we used equation (5) and the time-dependent record of δ^{13}C$_{\mathrm{atm}}$ described earlier.
- For (2), we applied an uncorrected value of δ^{13}C$_{\mathrm{wood}}$ (δ^{13}C$_{\mathrm{wood,uncorrrected}}$ = δ^{13}C$_{\mathrm{wood,corrected}}$ + δ^{13}C$_{\mathrm{atm}}$ – (−6.4‰)) to Equation (5).
- For (3), we computed Δ from W by combining equations (1) and (2) and solving for Δ as Δ = 4.4 + (27 – 4.4)(1 – 1.6W/c_a).
- For (4), we computed Δ by solving equation (2) for Δ as Δ = 4.4 + (27 – 4.4)c_i/c_a.

Physiological analysis of rate of change of *W* with *c*$_a$. We performed a theoretical analysis based on a physiological model of photosynthesis to interpret inferred changes in dW/dc_a over the twentieth century, in terms of the underlying physiological parameters that control photosynthesis. An approximate model for the biochemical dependence of the CO$_2$ assimilation rate, A, on intercellular CO$_2$ concentration, c_i, is given by equation (6):

$$A = A_{\max}\frac{c_{\mathrm{i}}}{c_{\mathrm{i}} + K} \tag{6}$$

where K is a biochemical parameter that depends on temperature, but otherwise is highly conservative across taxa. Equation (6) is equivalent to the biochemical model of Farquhar et al.[38], assuming that $A_{\max}$ is much greater the rate of mitochondrial respiration in the light (equation (3) also assumes this; compare it with equation (3) for C$_3$ plants in Box A from Ubierna et al.[37]). Combining equation (6) with the diffusional constraint on A ($A = g_{sc}(c_a – c_i)$) leads to a quadratic expression for c_i:

$$c_{\mathrm{i}}^2 + c_{\mathrm{i}}\left(\frac{A_{\max}}{g_{\mathrm{sc}}} - c_{\mathrm{a}} + K\right) - c_{\mathrm{a}}K = 0 \tag{7}$$

$W = A/g_{sw}$, where g_{sw} is the stomatal conductance to H$_2$O (g_{sw} = 1.6g_{sc}), is ($c_a – c_i$)/1.6, so dW/dc_a = (1 – dc_i/dc_a)/1.6 (also see equation (1)).

dW/dc_a, is found by implicitly differentiating equation (7) to give:

$$\frac{\mathrm{d}W}{\mathrm{d}c_{\mathrm{a}}} = \left(\frac{1}{1.6}\right)\frac{\frac{A_{\max}}{g_{\mathrm{sc}}} - c_{\mathrm{a}} + c_{\mathrm{i}}\left(1 + \frac{\mathrm{d}(A_{\max}/g_{\mathrm{sc}})}{\mathrm{d}c_{\mathrm{a}}}\right)}{\frac{A_{\max}}{g_{\mathrm{sc}}} - c_{\mathrm{a}} + 2c_{\mathrm{i}} + K} \tag{8}$$

Equation (8) indicates that, for a given c_i and c_a, variations in dW/dc_a are mainly driven by the ratio of photosynthetic capacity to stomatal conductance ($A_{\max}/g_{sc}$) and how that ratio changes in response to rising c_a (d($A_{\max}/g_{sc}$)/dc_a). The latter quantity can be estimated by applying estimates for c_a, c_i and K, and observed values of dW/dc_a to equation (8) under carboxylation-limited conditions, and assuming c_a = 297 (year 1900) or 370 ppm (year 2000), and c_i = 225 or 261 ppm (1901 or 2000, respectively, based on the mean W in our dataset of 45.0 and 66.6 ppm, respectively), and $K \approx$ 740 ppm (at 25 °C (refs [39,40])). Combining equation (6) with $A = g_{sc}(c_a – c_i)$ gives $A_{\max}/g_{sc} \approx$ 309 ppm in 1900 and 418 ppm in 2000, so that the respective dW/dc_a values are:

$$\left.\frac{\mathrm{d}W}{\mathrm{d}c_{\mathrm{a}}}\right|_{1900} \approx \frac{309 - 297 + 225\left(1 + \frac{\mathrm{d}(A_{\max}/g_{\mathrm{sc}})}{\mathrm{d}c_{\mathrm{a}}}\right)}{1.6(309 - 297 + 450 + 740)} = 0.006 + 0.117\left(1 + \frac{\mathrm{d}(A_{\max}/g_{\mathrm{sc}})}{\mathrm{d}c_{\mathrm{a}}}\right) \tag{9}$$

and

$$\left.\frac{\mathrm{d}W}{\mathrm{d}c_{\mathrm{a}}}\right|_{2000} \approx \frac{418 - 370 + 261\left(1 + \frac{\mathrm{d}(A_{\max}/g_{\mathrm{sc}})}{\mathrm{d}c_{\mathrm{a}}}\right)}{1.6(418 - 370 + 522 + 740)} = 0.023 + 0.125\left(1 + \frac{\mathrm{d}(A_{\max}/g_{\mathrm{sc}})}{\mathrm{d}c_{\mathrm{a}}}\right) \tag{10}$$

Applying dW/dc_a = 0.36 and 0.21 in 1900 and 2000 (Fig. 3b), respectively, gives d($A_{\max}/g_{sc}$)/dc_a as 2.02 and 0.50 in 1900 and 2000, respectively. Repeating the same calculations under RuBP (ribulose 1,5-bisphosphate)-regeneration-limited conditions, in which $K \approx 86\,\text{ppm}$, gives:

$$\left.\frac{\mathrm{d}W}{\mathrm{d}c_\mathrm{a}}\right|_{1900} \approx \frac{100-297+225\left(1+\frac{\mathrm{d}(A_\mathrm{max}/g_\mathrm{sc})}{\mathrm{d}c_\mathrm{a}}\right)}{1.6(100-297+450+80)} = -0.365+0.415\left(1+\frac{\mathrm{d}(A_\mathrm{max}/g_\mathrm{sc})}{\mathrm{d}c_\mathrm{a}}\right) \tag{11}$$

and

$$\left.\frac{\mathrm{d}W}{\mathrm{d}c_\mathrm{a}}\right|_{2000} \approx \frac{145-370+261\left(1+\frac{\mathrm{d}(A_\mathrm{max}/g_\mathrm{sc})}{\mathrm{d}c_\mathrm{a}}\right)}{1.6(145-370+522+80)} = -0.367+0.426\left(1+\frac{\mathrm{d}(A_\mathrm{max}/g_\mathrm{sc})}{\mathrm{d}c_\mathrm{a}}\right) \tag{12}$$

to give $\mathrm{d}(A_\mathrm{max}/g_\mathrm{sc})/\mathrm{d}c_\mathrm{a}$ as 0.74 in 1900 and 0.36 in 2000.

Effects of ontogeny. Brienen et al.[41] recently extended our knowledge of well-known ontogenic (height and age) effects on W for a few common tree species. They noted that height-related effects were strongest early in tree age (also known as the juvenile period effect), although they extended to as much as 50 years of age in some cases. All the described height effects[41] were strongly species specific. Brienen et al.[41] noted the difficulties involved in separating the effects of tree age from those of atmospheric CO_2, given that in most studies both increase contemporaneously. To make matters worse, any increase in time (years) is also an increase in respective tree age.

We carefully assessed the original sources and found utilizable tree age/height data for only 25 isotope series out of a total of 422. The present dataset also represents 134 species, of which only a few have specific height corrections. To apply generalized age/height corrections would introduce serious artefacts, given the large differences among species in observed height–W relationships[41]. The present dataset is dominated by isotope series from trees that were already well beyond the juvenile period prior to the twentieth century (many isotope series are >100 years of tree age). As shown by Brienen et al.[41], corrections for height become progressively smaller beyond around 50 years of age. For these reasons we did not attempt to correct the isotope data for tree age/height.

Although we could not correct for tree age/height, the assembled data provide indirect tests of such ontogenic effects. For example, the Great Depression of the 1930s, and the 1940s 'plateau' in the aftermath of World War II were periods when concentrations of atmospheric CO_2 grew slowly, if at all[20,21]. In these periods, $\mathrm{d}W/\mathrm{d}c_\mathrm{a}$ were greater than in any other period in the twentieth century (Fig. 4). We must bear in mind that the trees from which isotope data were derived were probably at least 40 years old by 1930, and at least 60 years old by 1950. If tree height was solely responsible for the observed $\mathrm{d}W/\mathrm{d}c_\mathrm{a}$, then these trees must have rapidly increased in height in both the 1930s and the late 1940s, yet changed little in height in the period between. Such ontogenic patterns have not been observed. Generally, height growth increases quickly during the 'juvenile period' before slowing, often markedly, by age 50 or so. There is also no evidence in the data presented by Brienen et al.[41] of a rapid increase in age/height effects towards middle age.

We cannot exclude possible contributions of height and age to increases in W recorded in the first few decades of some individual isotope series, but the likely effects are small in contrast to the dominant effect of c_a in the mature trees that comprise the bulk of the present dataset.

Although we agree with Brienen et al.[41] (and a great many other authors) that tree height and age influence isotopic abundances during the early decades of tree growth, this effect has been known for many years and is well accounted for within the long-term data presented here. Many authors of tree-ring studies actually explicitly excluded data from the first few decades (that is, reported isotope series that commence after 20 or 30 years of tree growth).

Statistical analysis. Isotopic data in the literature extend back hundreds of years in the cases of very long-lived trees (mainly conifers, See Supplementary Table 1). Although we compiled the isotope data from 1850 onwards, we also focused a detailed analysis of $\mathrm{d}W/\mathrm{d}c_\mathrm{a}$ on isotope series that spanned 1901–2000. For some decadal analyses, we extended the range of analysis to 2010 so as to capture the latest available data.

We used simple regression analyses to assess $\mathrm{d}W/\mathrm{d}c_\mathrm{a}$ for all the isotope series. We identified differences between the $\mathrm{d}W/\mathrm{d}c_\mathrm{a}$ of angiosperms and gymnosperms and the Köppen climates for all the data available, and for discrete time periods (for example, decades) using linear mixed models (with individual studies as the random variable). We also examined the influence of climate variables (average mean annual precipitation, mean annual potential evaporation, mean annual temperature, vapour pressure and radiation between 1900 and 2000) on $\mathrm{d}W/\mathrm{d}c_\mathrm{a}$ for both angiosperms and gymnosperms with regression analyses. All statistical analyses were completed with SPSS or R.

Data availability

The data for W can be accessed via the Zenodo repository (https://doi.org/10.5281/zenodo.3693240). Source data for Fig. 1 are provided with the paper.

Code availability

The code used in processing data can be accessed via the Zenodo repository (https://doi.org/10.5281/zenodo.3693240).

References

34. McCarroll, D. & Loader, N. J. Stable isotopes in tree rings. *Q. Sci. Rev.* **23**, 771–801 (2004).
35. Robertson, A. et al. Hypothesized climate forcing time series for the last 500 years. *J. Geophys. Res.* **106**, 14783–14803 (2001).
36. Keeling, C. D. et al. in *A History of Atmospheric CO_2 and its effects on Plants, Animals and Ecosystems* (eds Ehleringer, J. R. et al.) 83–113 (Springer, 2005).
37. Ubierna, N. Holloway-Phillips, M.-M. & Farquhar, G. D. in *Photosynthesis—Methods and Protocols* (Ed. Covshoff, S.) 155–196 (Humana Press, 2018).
38. Farquhar, G. D. et al. A biochemical model of photosynthetic CO_2 assimilation in leaves of C_3 species. *Planta* **149**, 78–90 (1980).
39. Wong, S. C. et al. Stomatal conductance correlates with photosynthetic capacity. *Nature* **282**, 424–426 (1979).
40. De Pury, D. G. G. & Farquhar, G. D. Simple scaling of photosynthesis from leaves to canopies without the errors of big-leaf models. *Plant Cell Environ.* **20**, 537–557 (1997).
41. Brienen, R. J. W. et al. Tree height strongly affects estimates of water-use efficiency responses to climate and CO_2 using isotopes. *Nat. Commun.* **8**, 288 (2017).

Acknowledgements

We thank the authors who provided additional information that allowed us to include their data in this work. We thank A. Barlow for help with digitizing the isotope series and M. Gharun for help with climate data. M.A.A. and T.L.T. thank the Australian Research Council for general support. M.A.A. thanks an anonymous donor for funding of this study. T.N.B. acknowledges support from the National Science Foundation (grant no. 1557906) and the USDA National Institute of Food and Agriculture (Hatch project 1016439).

Author contributions

M.A.A., T.L.T. and T.N.B. developed the original ideas included in this paper. T.L.T. screened the literature, led the extraction of data and characterized the dataset. T.N.B. interrogated the dataset for analysis and prepared the modelling. T.L.T. analysed the data and prepared the figures and tables. M.A.A. wrote the paper with T.L.T. and T.N.B.

Competing interests

The authors declare no competing interests.

Additional information

Extended data is available for this paper at https://doi.org/10.1038/s41558-020-0747-7.

Supplementary information is available for this paper at https://doi.org/10.1038/s41558-020-0747-7.

Correspondence and requests for materials should be addressed to M.A.A.

Peer review information Nature Climate Change thanks Katrin Fleischer and the other, anonymous, reviewer(s) for their contribution to the peer review of this work.

Reprints and permissions information is available at www.nature.com/reprints.

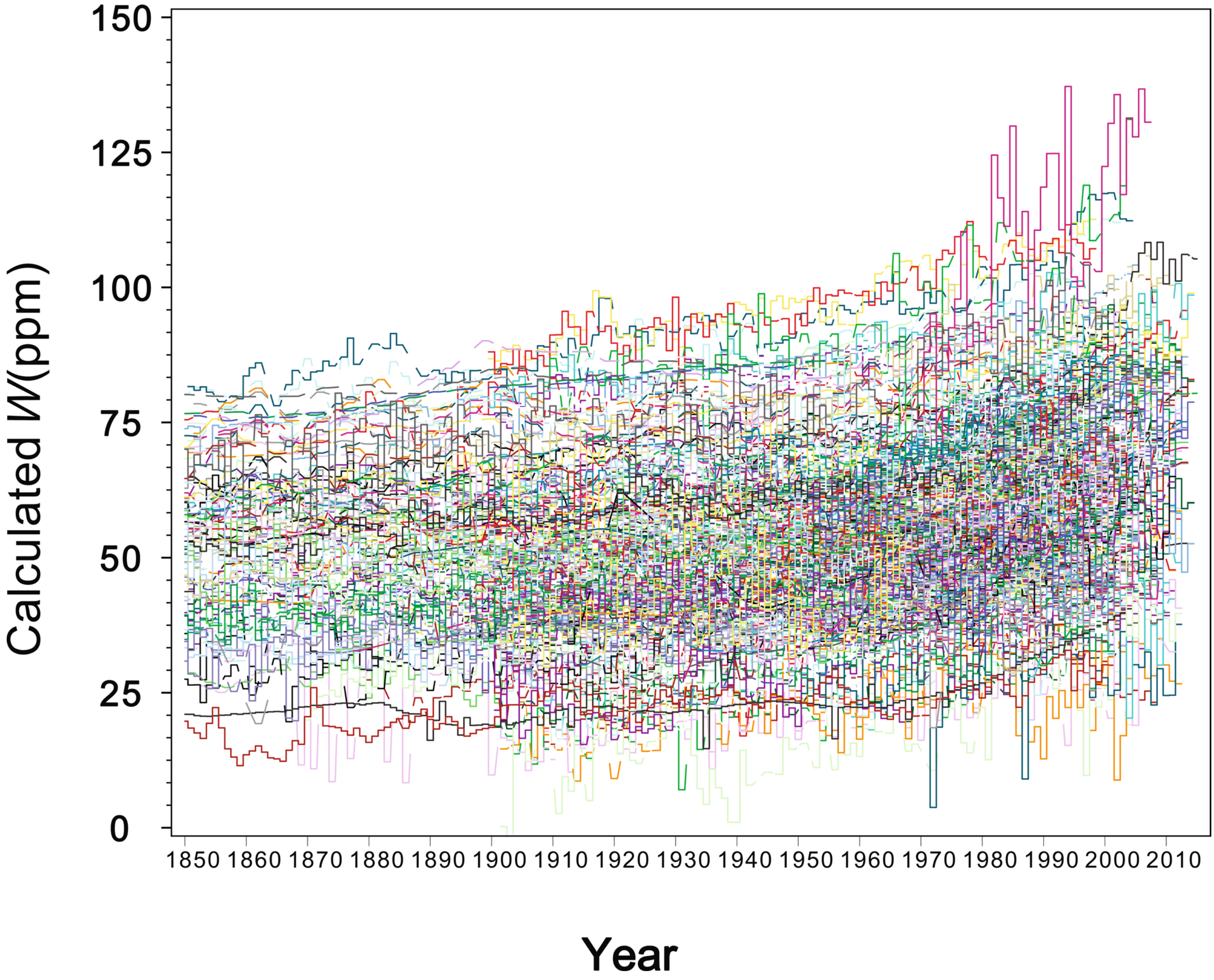

Extended Data Fig. 1 | Relationship of *W* to sample year. For all 422 tree-ring isotope series containing data from the period 1851–2015, *W* was calculated using Equation 3.

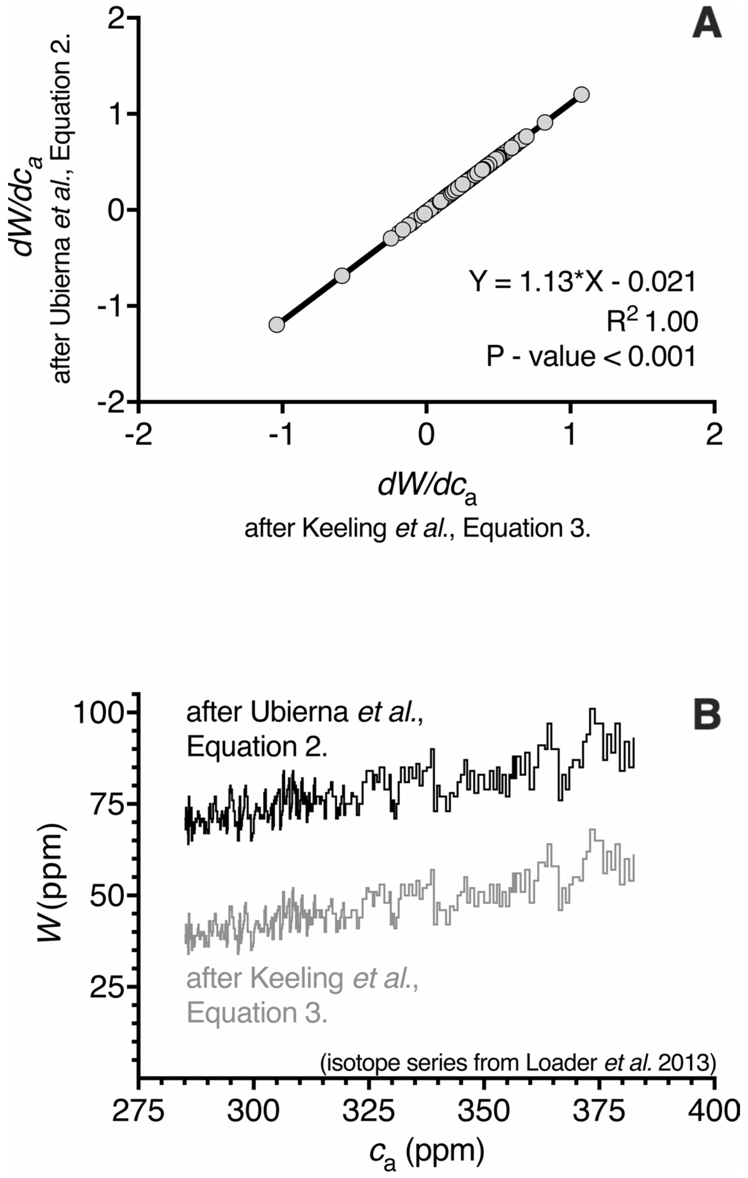

Extended Data Fig. 2 | Effects of methods of calculation of *W*. a, Relationship between dW/dc_a calculated using Equation 2 with that calculated using Equation 3 (based on $^{13}C/^{12}C$ ratios of wood tissue for all series shown in Extended Data Fig. 1. **b**, Example of the difference in calculated *W* if either Equations 2 or 3 are applied to isotope data as extracted from Loader *et al.*[42].

42. Loader, N. J. et al. Stable carbon isotopes from Torneträsk, northern Sweden provide a millennial length reconstruction of summer sunshine and its relationship to Arctic circulation. *Q. Sci. Rev.* **62**, 97–113 (2013).

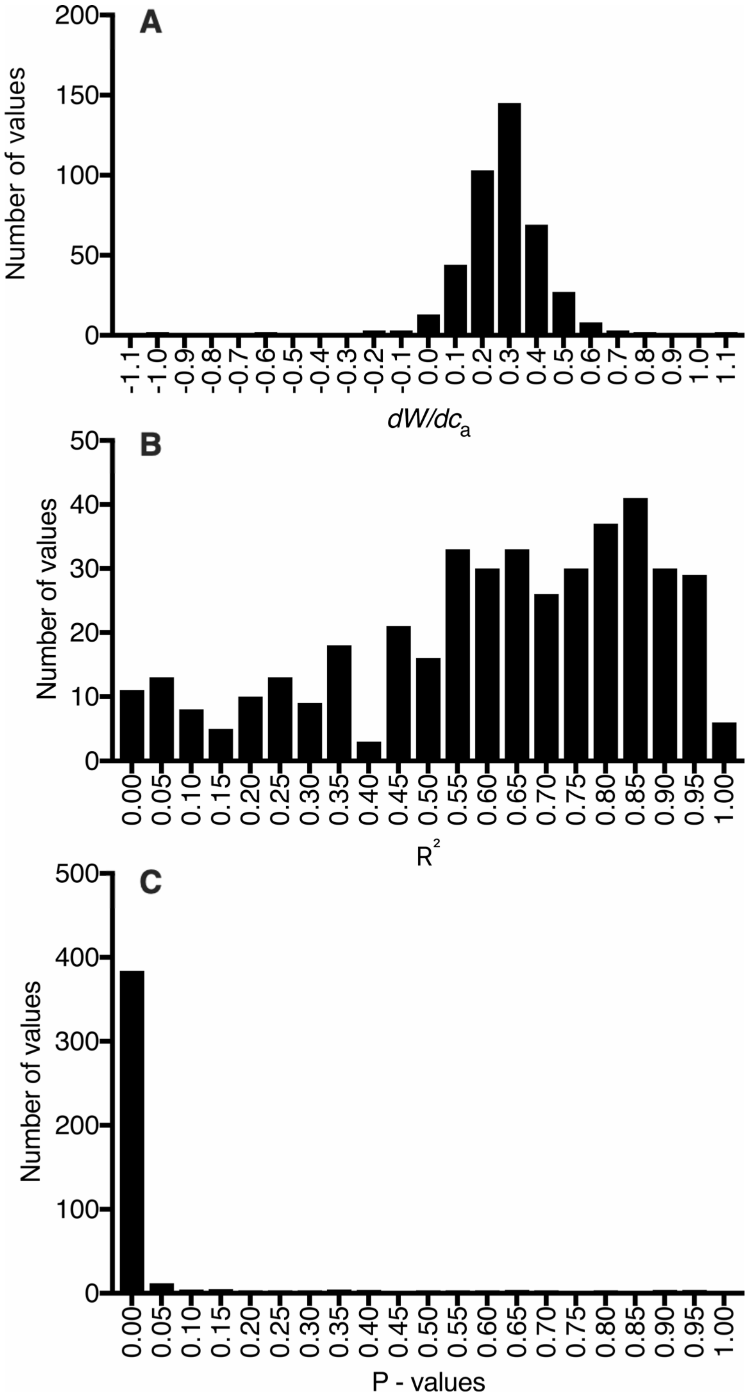

Extended Data Fig. 3 | Descriptive statistics for the global dataset of rates of change in W with c_a (dW/dc_a). Data are as shown for Extended Data Fig. 1. **a**, Frequency of dW/dc_a. **b**, Frequency of R^2 values for relationships between W and c_a. (**c**) Frequency of P-values for relationships between W and c_a.

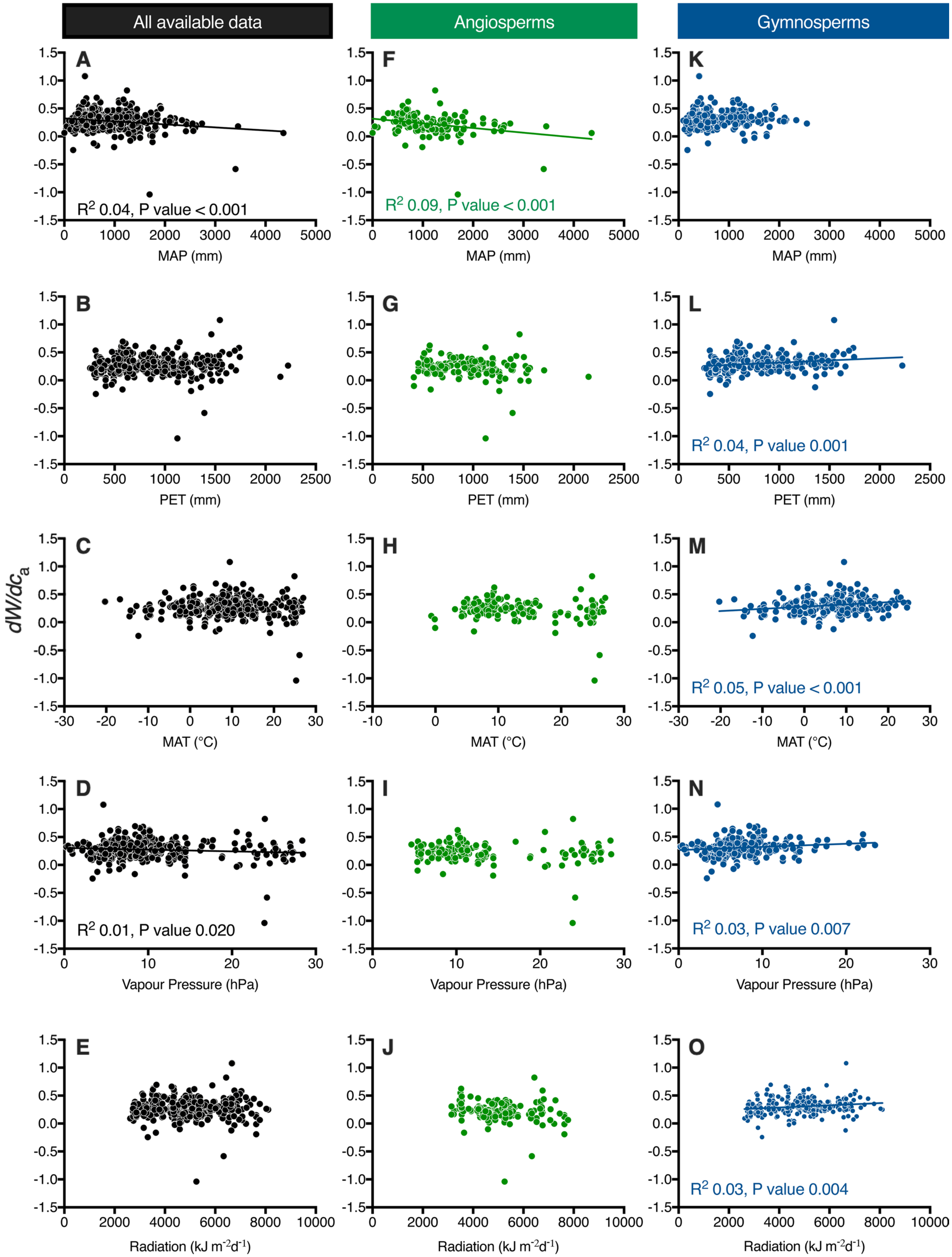

Extended Data Fig. 4 | Effects of climatic variables on rates of change in *W* with c_a (dW/dc_a). Linear regressions of dW/dc_a and climatic variables: mean annual precipitation, MAP; potential evapotranspiration, PET; mean annual temperature, MAT; vapour pressure; and radiation. (**a–e**) All data as shown in Extended Data Fig. 1. (**f–o**) Angiosperms (n = 147) and gymnosperms (n = 275) considered separately.